

Color Change of Tourmaline by Heat Treatment and Electron Beam Irradiation: UV-Visible, EPR, and Mid-IR Spectroscopic Analyses

Apichate MANEEWONG

*Korean University of Science & Technology, Daejeon 34113, Korea,
Neutron Science Division, Korea Atomic Energy Research Institute, Daejeon 34057, Korea and
Gems Irradiation Center, Thailand Institute of Nuclear Technology, Onkharak, Nakhon-Nayok 26120, Thailand*

Baek Seok SEONG*

*Korean University of Science & Technology, Daejeon 34113, Korea and
Neutron Science Division, Korea Atomic Energy Research Institute, Daejeon 34057, Korea*

Eun Joo SHIN

Neutron Science Division, Korea Atomic Energy Research Institute, Daejeon 34057, Korea

Jeong Seog KIM

Department of Digital Display Engineering, Hoseo University, Asan 31499, Korea

Varavuth KAJORNRIITH

Gems Irradiation Center, Thailand Institute of Nuclear Technology, Onkharak, Nakhon-Nayok 26120, Thailand

(Received 26 January 2015)

The color of pink tourmaline gemstone changed to colorless when heating at temperature of 600 °C in air. This colorless tourmaline recovered its pink color when irradiated with an electron beam (e-beam) of 800 kGy. The origin of the color change was investigated in three types of tourmaline gemstones, two pink are from Afghanistan and one green are from Nigeria, by using Ultraviolet-visible spectroscopy (UV-Vis), Fourier-transform infrared spectroscopy (FTIR), Electron paramagnetic resonance (EPR), and Energy Dispersive X-ray Fluorescence (EDXRF). The UV-Vis absorption spectrum of the pink tourmaline with higher Mn concentration (T2, 0.24 wt%) showed characteristic absorption peaks originating from the Mn³⁺ color center: two absorption bands centered at wavelength of 396 and 520 nm, respectively. Both absorption bands disappeared when heated in air at 600 °C and then reappeared when irradiated with an e-beam at 800 kGy. EPR T2 spectra showed that the color change was related to the valence change of Mn³⁺ to Mn²⁺ and vice versa. The pink tourmaline of lower MnO content (T1, 0.08 wt%) also became colorless when heated, but the color was not recovered when the gemstone underwent e-beam irradiation. Instead, a yellow color was obtained. UV-Vis and FTIR spectra indicated that this yellow color originated from a decomposition of the hydroxyl group (–OH) into O[–] and H^o by the e-beam irradiation. Green tourmaline did not show any color change with either heat treatment or e-beam irradiation.

PACS numbers: 33.35.+r, 61.80.Fe, 81.40.Gh, 82.80.Ej

Keywords: Tourmaline, Heat treatment, Electron irradiation, UV-Vis, EPR, FTIR

DOI: 10.3938/jkps.68.83

I. INTRODUCTION

Tourmaline is a group of chemically complex borosilicate minerals that show a variety of colors; two or more colors are observed even in the same crystal [1]. It can be represented by the general formula

$XY_3Z_6(BO_3)_3(T_6O_{18})V_3W$ [2], where the X is a 9 coordination number (CN) site occupied by Na⁺, Ca²⁺, K⁺ and a partial vacancy; the Y is 6 CN site (octahedral polyhedron) occupied by Li⁺, Mg²⁺, Fe²⁺, Mn²⁺, Al³⁺, Fe³⁺, Cr³⁺, V³⁺, Mn³⁺ and Ti⁴⁺, which are expressed as ^YM in the present work; the Z is 6 CN site (octahedral) consisting mostly of Al³⁺ and with minor impurities of Fe³⁺, Mg²⁺, Cr³⁺ and V³⁺, which are ex-

*E-mail: bsseong@kaeri.re.kr; Fax: +82-42-868-4629

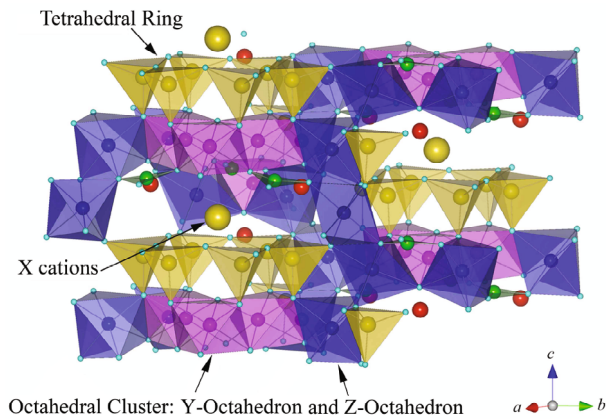


Fig. 1. (Color online) Structure of tourmaline (T1).

pressed as ${}^Z\text{M}$; T is tetrahedral site (4CN) occupied by Si^{4+} , with a small amount of Al^{3+} ; B is a 3 CN site occupied by B^{3+} ; the V site is mainly occupied by OH^- and O^{2-} ; the W site is occupied by OH^- , O^{2-} and F^- .

The optical properties of tourmaline are frequently governed by a cluster of transition-metal cations located in the octahedral-Y sites which are octahedra that faces with each other. As shown in Fig. 1, a cluster of Y octahedra is connected to three smaller Z octahedra along the edge. Both units serve as linkages along a three-fold screw axis. The type, ordering and distribution of cations occupying in the Y and the Z sites in the octahedral clusters also affect the crystal fields of the Mn and the Fe ions.

Heat treatment is most commonly used to alter the color and to increase the clarity of gemstones. In tourmaline, heating can sometimes change overly dark pink stones to a lighter tone. It can also affect the color in other types of tourmaline (*i.e.*, dark green and brownish-red tourmalines). Some previous studies reported the effect of heat treatment. Heating at 600 °C can remove both the natural and the irradiation-induced pink color in elbaite (most of the multi-colored tourmalines are of the elbaite variety) [3,4]. In addition, heat treatment in air at 700 °C for 48 h of blue tourmaline can produce a red color due to oxidation of ferrous iron at the octahedral site and simultaneous to the trapping of excess electron [5]. Recently, heat treatment was performed on schorl (black tourmaline) [6]. The black color changed to brown at 700 °C and to reddish brown at 900 °C mainly due to oxidation of Fe. Although, effect of thermal treatment has been reported in several studies, color enhancement was not achieved due to the complex structure of tourmaline.

High-energy ionizing radiation also has the ability to change the color of various minerals, and a variety of damage centers can be induced by the irradiation process. X-ray /gamma irradiation is one popular method that has been used for a long time to enhance the color of tourmaline. Many previous studies have clearly re-

ported color changed by X-ray and gamma-ray exposure [4,7–15]. In contrast, the effect of e-beam irradiation has been pointed out only in one literature [16]. The effect of an electron beam on tourmaline is rarely reported.

In this research, we studied the color change of pink and green tourmaline, especially focusing on the color recovery mechanism due to e-beam irradiation after heat treatment. The mineralogical study on all sample crystals was carried out with a variety of techniques, especially energy dispersive X-Ray fluorescence (EDXRF) spectrometer, X-ray powder diffraction (XRD), UV-Vis spectroscopy, electron paramagnetic resonance (EPR) measurement and Fourier-transform infrared (FTIR) spectroscopy. The combination of these techniques allowed the chemical characterization of the tourmaline samples to delineate the origin of the color and the color change caused by e-beam radiation and heat treatment.

II. EXPERIMENTAL METHODS

1. Chemical Composition Analysis, Heat Treatment, and Electron Irradiation

Two pink tourmalines from Nigeria and one green tourmaline from Afghanistan were investigated. Each sample was cut in half perpendicular to the crystallographic *c*-axis. Subsequently, all samples were polished by using silicon-carbide abrasive paper. The evolution of the colors of the polished tourmaline samples with the heat treatment and the e-beam irradiation was studied.

The Eagle-III μ Probe from EDAX, a new generation of X-ray micro-fluorescence (XRMF) spectrometer, was used for analyzing major oxides and trace elements in the three samples. The spectrometer was installed at the Department of Mineral Resources at the Ministry of Natural Resources and Environment, Thailand. The sample was excited by X-rays (Rh tube) focused by a polycarpellary fiber lens to a minimum spot size of 50 microns. The energy-dispersive liquid-N₂-cooled Si detector with a Be window, suitable for detecting the XRF from chemical elements ranging from Na to U. Table 1 shows the analyzed chemical compositions of the three samples.

The polished natural gemstone samples were heated at 400 and 600 °C in air for 3 h. The heating rate to achieve these holding temperatures was 100 °C/hr. After heat treatment, the samples were cooled in the furnace.

The electron accelerator used in this study is located at the Gems Irradiation Center, Thailand Institute of Nuclear Technology (TINT), and can produce high-energy 5 – 20 MeV and a high power 10 – 20 kW. The accelerators power in kW is an important parameter for the processing rate/time of an electron beam exposed to gemstone. All samples were irradiated a 10 kW for 5 h to get an 800 kiloGray (kGy) dosage. Another important parameter is the energy in MeV, which indicates the

Table 1. Chemical compositions of the three tourmaline sample as measured by using EDXRF analyses.

Sample no.	T1 pink	T2 pink	T3 green
<i>Oxide:</i> (wt%)			
SiO ₂	37.20	36.87	34.61
Al ₂ O ₃	42.10	41.26	36.73
MgO	2.19	2.23	2.05
Na ₂ O	0.48	0.75	0.71
K ₂ O	0.04	0.03	0.04
CaO	0.08	0.18	1.47
TiO ₂	0.01	0.01	0.09
Cr ₂ O ₃	0.01	0.01	Nd
MnO	0.08	0.24	2.59
ZnO	Nd	Nd	0.55
FeO	0.02	0.03	5.70
F	2.59	2.68	1.98
B ₂ O ₃ *	11.01	10.91	10.71
Li ₂ O*	1.20	1.26	1.11
H ₂ O*	2.57	2.50	2.75
Subtotal	99.36	98.95	101.09
O=F	1.09	1.13	0.83
Total	98.27	97.82	100.26

* B₂O₃, Li₂O and H₂O calculated based on the stoichiometry, nd = not detected

penetration of the electrons passing through the stones; a higher energy will generate a higher penetration. The electrons need to pass through and out of the stone after they have induced the coloring effect. A suitable energy rang for small and medium stones are 8 – 10 MeV, and 20 MeV is suitable for larger stones. All our small samples were irradiated by using 8-MeV electrons. Electrons with low energy do not induce radioactivity in the tourmaline samples, so radioactivity decay process is not necessary. However, due to the increase in the sample's temperature induced by the application of high power to the stones during the electron-beam processing, cooling the stones is important. In our case, water was used for the cooling process. The tourmaline samples were either placed in moving water or sprayed with water during the processing.

2. X-ray Powder Diffraction (XRD)

The crystal phases of all samples were investigated using X-ray powder diffraction. The X-ray powder diffraction data were collected by using an Empyrean PIXcel3D diffractometer equipped with an X-ray tube (Cu K_α ra-

diation: $\lambda = 1.540598 \text{ \AA}$; 30 kV, 15 mA) and a diffracted beam graphite monochromator at the Korea Atomic Energy Research Institute (KAERI), Daejeon, South Korea. The specimen was scanned from $10 - 120^\circ 2\theta$, with a step size of 0.02° and a counting time of 1 second per step.

3. UV-Vis Spectroscopy (UV-Vis)

UV-Vis spectroscopic measurements on the platelets oriented parallel and perpendicular to the *c*-axis were measured before and after irradiation. An UV-Vis spectroscopy analysis was performed by using the PerkinElmer lambda 750 UV-Vis-NIR spectrophotometer located at the Gems Irradiation Center, Ongkharak Branch, TINT. UV-Vis spectra were recorded in the wavelength region of 200 – 800 nm at a scanning speed of 200 nm/min.

4. Electron Paramagnetic Resonance (EPR)

The tourmaline samples prepared for the EPR studies were ground into fine powder in a mortar. All EPR measurements were performed at room temperature on a Bruker EPR spectrometer (ESP 300 series) operated at an X-band microwave frequency at the Seoul Branch of the Korea Basic Science Institute. The spectrometer's operating conditions adopted during the experiment were a 350.0-mT central magnetic field, a 140- to 600-mT scan ranges, a 9.64-GHz microwave frequency, a 1.0-mW microwave power, a 100-kHz field modulation frequency, a 1.0-mT field modulation amplitude and a 0.02-s time constant. 1, 1-diphenyl-2-picrylhydra-2l (DPPH) with a *g* factor of 2.0036 was used as an internal standard for *g*-factor calculations. After the spectra had been measured, the positions of the EPR signals were labelled by using their effective *g* (g_{eff}) values. The g_{eff} was calculated by using the relationship, $g_{eff} = h\nu/\beta H$, where h , ν , β , and H are Planck's constant, the microwave frequency, the electron Bohr magneton and the external field, respectively. The linewidth (ΔB_{pp}) of each signal was also observed.

5. Fourier-Transform Infrared Spectroscopy (FTIR)

The mid-infrared spectra of the tourmaline samples were recorded in the range from 400 to 5000 cm⁻¹ by using a Bruker ALPHA Spectrometer with 100 scans and 4-cm⁻¹ resolution at the Department of Mineral Resources

Table 2. (Color online) Heat treatment results for the three samples.

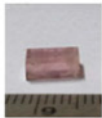

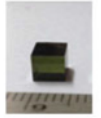




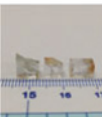
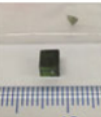

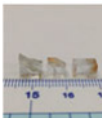
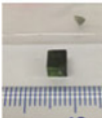



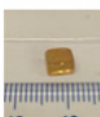


Temp	T1	T2	T3
0 °C (natural)			
	Pale pink	Pale pink	Dark green
400 °C			
	Slightly lighter	Slightly lighter	No change
600 °C			
	Colorless	Colorless	No change

Table 3. (Color online) E-beam irradiation results for the samples.

Absorbed Dose	T1	T2	T3
0 kGy (after heating at 600 °C for 3 h)			
	Colorless	Colorless	Dark green
600 kGy			
	Pink-yellow	Pale pink	No change
800 kGy			
	Yellow	Deep pink	No change

under the Ministry of Natural Resources and Environment, Thailand. Band fittings were done with Gauss-Lorentz functions by using the fitting program Origin 8.0.

III. RESULTS AND DISCUSSION

1. Chemical Composition and Color Change Results

The chemical compositions of the three tourmaline samples are shown in Table 1. The EDXRF analysis indicated that all tourmalines T1, T2 and T3, were fluor-elbaite with fluorine weight fraction, of 2.59%, 2.68% and 1.98%, respectively. They contained significant amounts of MgO and MnO, and a small quantity of FeO. The T3 sample (green) had a large amount of FeO, 5.70%. Cr₂O₃ and ZnO existed as impurities. The T2 pink tourmaline had a higher amount of MnO than the T1 pink tourmaline. T3 contained very high amounts of MnO and FeO.

The results of the heat treatments regarding color change of the samples are summarized in Table 2. At 400 °C all three samples showed almost no change. After heating at 600 °C the two pink samples showed big change; they became colorless. However, the green one still remained the same color as before the heat treatment.

Table 3 shows the effect of e-beam irradiation on the color of the three samples that were heat treated at 600 °C. When irradiated with electrons at 400 kGy, the two colorless tourmalines partially recovered their pink color. T1 displayed a pink-yellow color whereas T2 become a shade of pink close to pink color of its natural state. T3 still did not show any color change. When e-beam dosage was increased to 600 kGy, the pink-yellow color in T1 changed to yellow. On the other hand, T2 completely recovered its original pink color. Again, T3 showed no changes in color.

2. XRD Patterns Analysis

In order to investigate any crystal structural change induced by heat treatment or e-beam irradiation, X-ray diffraction (XRD) patterns for three tourmaline samples were taken and the results are given in Fig. 2. As expected, all three samples had hexagonal structure with space group R3m. The XRD patterns of these tourmalines matched the pattern of a representative fluor-elbaite sample (RRUFF ID: R130035). The samples that were heated at 600 °C and underwent e-beam irradiation at 800 kGy did not show any significant changes.

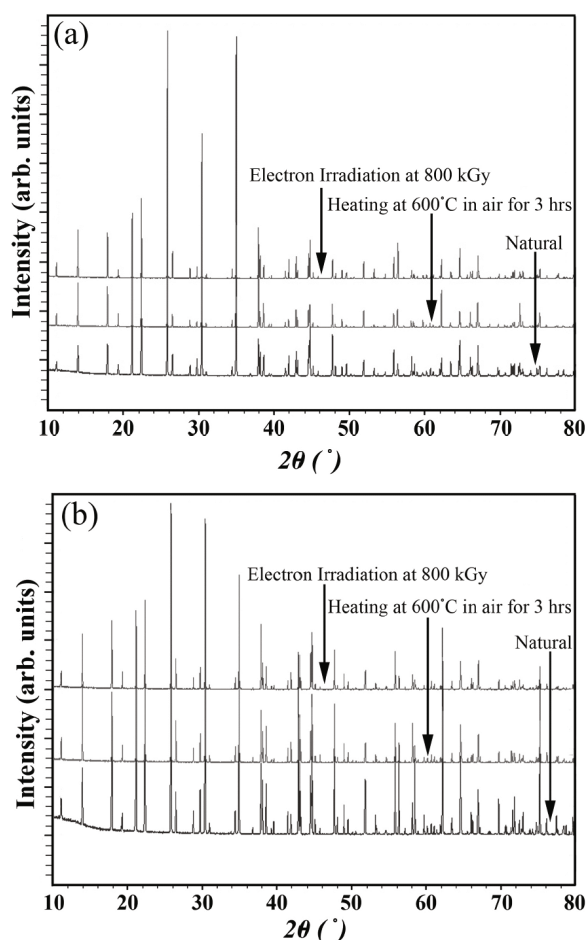


Fig. 2. Powder XRD patterns for the natural state and the state after treatment of: (a) T1, (b) T2 and (c) T3.

3. UV-Vis Spectra Analysis

UV-Vis spectroscopy is a powerful tool for studying the color of minerals containing transition metals. The UV-Vis absorption spectra ($E \perp c$) of the two pink tourmalines (T1 and T2) are presented in Figs. 3(a) and (b), respectively. Both natural pink tourmalines showed broad absorption bands at 396 and 520. After they had been heated at 400 °C, the intensities of the absorption bands at 396 and 520 of both pink tourmalines have decreased (dashed line). When they were heated at 600 °C, these peaks disappeared (square-symbol line), which conformed to the disappearance of color in both samples.

Figure 3(a) shows the absorption spectra of T1 after e-beam irradiation, which appears to have a yellow color. With an electron dose of 600 kGy, a small broad absorption band reappears at 520 nm (circle-symbol line). In particular, the base line of the absorption spectrum over the range of 300 ~ 550 nm is steeply increased by e-beam irradiation. With increasing e-beam dosage to 800 kGy, the base line appears to be the same as that of the 600 kGy sample. The two absorption peaks, one

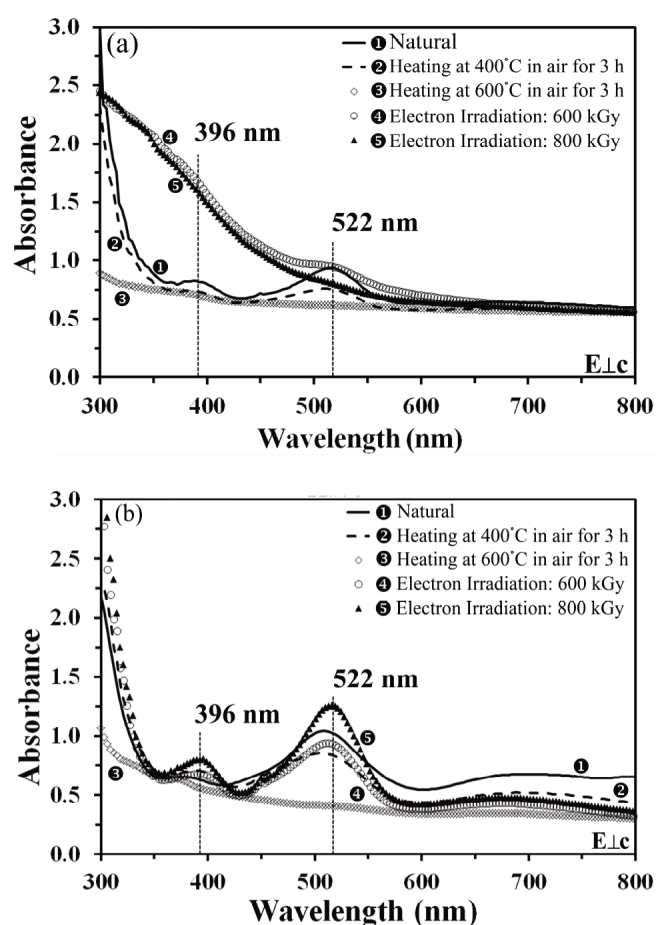


Fig. 3. UV-Vis spectra of the two pink tourmalines: (a) T1 and (b) T2.

each 396 and 520 nm, were overridden by the increase in the background over the range from 300 to ~ 550 nm. The yellow color of the e-beam-irradiated T1 can be ascribed to the drastic increase in the background line of the absorption spectrum from 300 to ~ 550 nm. These absorption peaks actually exist in the e-beam-irradiated samples (triangle- and open-circle symbols).

Recovery of the pink color due to e-beam irradiation of the colorless T2 (after heating) can be confirmed by the absorption spectrum shown in Fig. 3(b). After heat treatment, the two absorption bands, 396 and 520 nm, disappear, but when irradiated with an e-beam (400 kGy), these two absorption peaks reappear, and their intensities increased when the dosage was raised to 600 kGy (triangle-symbol line).

Several interpretations for the two bands, 396 and 520 nm, have been suggested. Both absorption bands can come from Mn^{3+} and/or Mn^{2+} - Mn^{3+} [13,17–19]. First, these absorption bands in natural pink samples cannot originate from Mn^{2+} because the d-d electronic transition of Mn^{2+} (d^5 configuration) is spin-forbidden; hence, it has very low absorption coefficients [20]. On the other hand, Mn^{3+} (d^4 configuration) has a strong absorption

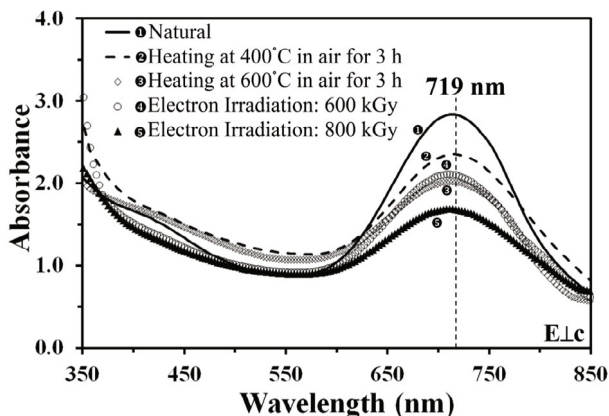


Fig. 4. UV-Vis spectra of the T3 sample.

coefficient because its electronic transition is permitted and the crystal field is very asymmetric due to the compressed octahedron at Y site along the $\text{OH}_1\text{-OH}_3$ axis [16].

The exchange coupling among the Mn (Fe) ion pairs in two different sites (Y and Z) can also produce a pink-red (yellow) color, as suggested by Mattson *et al.* [21]. The Fe^{3+} -rich tourmaline shows intense optical absorption features at 485 and 540 nm caused by exchange coupling between Fe^{3+} clusters. After heating at 400 °C for 3 h in air, pink samples became a slightly lighter pink and then became colorless when the temperature was increased to 600 °C. These results can be ascribed to the reduction of Mn^{3+} to Mn^{2+} by the heat treatment.

With electron irradiation at 600 kGy, T1 displayed a pink-yellow color and then changed to yellow when the electron dose was increased to 800 kGy. This color change to yellow both at 600 and 800 kGy can be ascribed to a substantial increase in the background in the absorption spectrum (300- ~ 550-nm range, Fig. 3). This absorption background has been suggested by Krambrock *et al.* [22] to be due to O^- hole trap centers located at the OH site. If tourmaline is irradiated by an electron beam, the OH^- molecule in the OH site will be decomposed into O^- (hole trap) and H° (electron trap). In contrast, T2 recovered its deep pink color upon e-beam irradiation at an 800-kGy dosage. In T2, the background of the absorption spectrum remained the same as before e-beam irradiation. This indicates that the OH group was not decomposed by e-beam irradiation. The two strong absorption bands at 390 and 520 nm in T2 reappeared due to the irradiation, which indicates that Mn^{2+} ions oxidized to Mn^{3+} .

Figure 4 shows absorption spectra ($E \perp c$) of green tourmaline (T3). After the heat treatment, the absorption maxima in the vicinity of 700 nm were slightly decreased. The intensity of this broad absorption band decreases further due to e-beam irradiation at a dosage of 800 kGy. Even with the slight decrease in the intensity of the absorption spectrum, the color remained the

same.

The absorption maximum in the vicinity of 700 nm in green tourmaline has been reported in several previous works [23–26]. This band occurs due to presence of Fe^{2+} or Cu^{2+} that produces a greenish blue color. Because no Cu ions (Table 1) are present in T3, one possible reason for the intensity decrease of the absorption band (~ 700 nm) may be the exchange interaction $\text{Fe}^{2+} \leftrightarrow \text{Fe}^{3+}$, as suggested by Ahn *et al.* [16]. Partial oxidation of Fe^{2+} seems to occur during heat treatment in air, where oxidation can decrease the intensity of the absorption band at 700 nm. After subsequent e-beam irradiation, the intensity of this band was slightly increased. However, the oxidation/reduction reactions produced by these treatments are not enough to change the color of T3. Another atmosphere such as heated nitrogen gas, and diffusion treatment may be more suitable, as suggested by Castañeda *et al.* [5].

4. EPR Analysis

EPR was used in this study for investigating the chemical status of the paramagnetic ions Fe^{3+} , Mn^{2+} and their valence change upon heating and electron irradiation. The X-band EPR spectra of T1 and T2 are shown in Figs. 4(a) and (b), respectively. All investigated samples exhibited resonance signals. The natural state of T1 (green line in Fig. 5(a)) showed a relatively sharp signal at $g \approx 2.0$ (with linewidth $\Delta B_{pp} = 4 - 5$ mT) and a very broad peak at $g \approx 3.5$ ($\Delta B_{pp} = 35 - 40$ mT). The resonance signal of standard sample appeared at g 1.87 and 2.17. The green line (natural T2) in Fig. 5(b) showed a relatively sharp signal ($\Delta B_{pp} = 4 - 5$ mT) at $g \approx 2.07$ and a broad peak at $g \approx 3.5$ ($\Delta B_{pp} = 35 - 40$ mT), as well as six hyperfine lines for $g \approx 2.07$. EPR spectra of T3 were different from those of T1 and T2. Due to the high concentrations of Mn (2.59%wt) and Fe (5.70%wt), broad resonance signals appeared.

Several previous reports in the literature have reported on the resonance signals due to Fe and Mn ions. Fe^{2+} ($3d^6$) is a non-Kramers ion [27] and is generally unobservable by using EPR [28]. In contrast, Fe^{3+} ($3d^5$) has been extensively studied in a wide range of materials. In an environment that is close to a cubic symmetry, resonances at or near $g \approx 2.0$ are expected. The Mn^{2+} ion has an unpaired electron configuration $3d^5$ so that, in general, there are six spin levels ($S = \pm 5/2, \pm 3/2, \pm 1/2$). In addition, the spin of the ^{55}Mn nucleus ($I = 5/2$) results in six hyperfine lines. Several previous reports in the literature on the EPR spectra of Mn^{2+} in various materials indicate signals at $g \approx 2.0$, $g \approx 2.5$, $g \approx 3.5$, and $g \approx 4.3$, as well as the six hyperfine lines [29–32]. Fe^{3+} also showed resonance signals at $g \approx 2.0$, $g \approx 4.3$, $g \approx 6.0$ and $g \approx 10.0$ [33–35]. Recent EPR studies on tourmaline (Fe-poor elbaite) assigned signals at $g \approx 2.5$ and 3.5 to Mn^{2+} and signals at $g \approx 4.3$ and 2.0 to

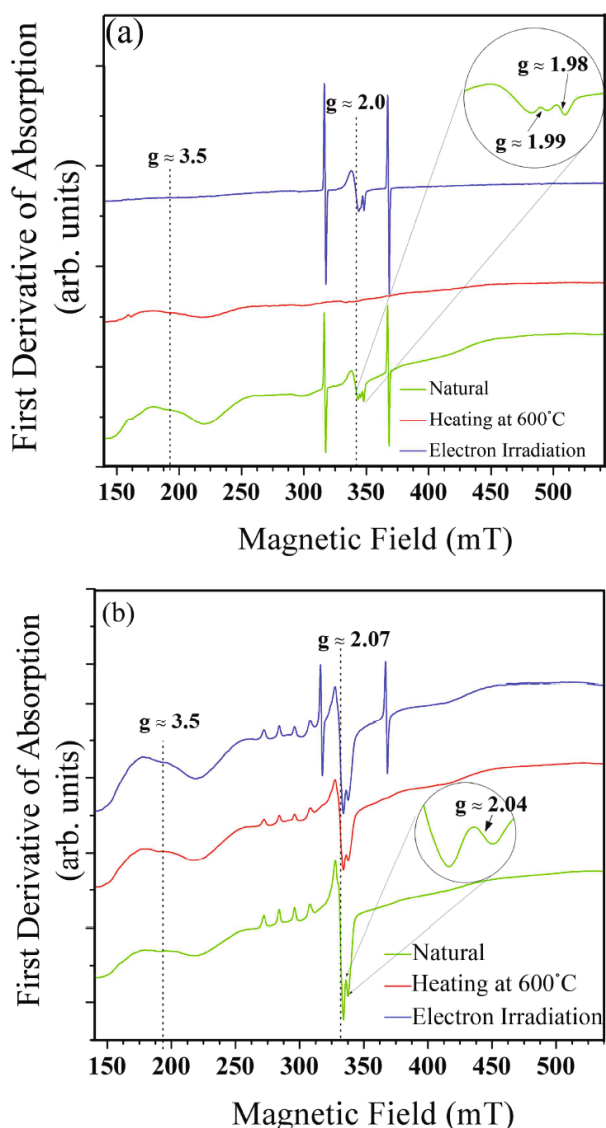


Fig. 5. (Color online) EPR Spectra of (a) T1 and (b) T2.

Fe^{3+} [36].

The EPR spectra of T1 and T2 in their natural states (green lines in Figs. 5(a) and (b)) indicated that the signals at $g \approx 2.0$ and 3.5 correspond to Mn^{2+} and/or Fe^{3+} . The signal at $g \approx 2.0$ (T1, T2) can be attributed to isolated Mn^{2+} and/or Fe^{3+} ions in a strongly-distorted surrounding octahedron. The broad signal at $g \approx 3.5$ can be related with magnetically-coupled clusters of Mn^{2+} -O- Mn^{3+} or Mn^{2+} -O- Fe^{3+} [37]. The Fe^{3+} affects the observed EPR signals to a lesser degree than the Mn^{2+} does due to the low content of Fe in both pink samples (see in Table 1). The insets (in Fig. 5) show additional small signals at $g \approx 2.0$. These small signals might come from Fe^{3+} . In T1, the resonance signals at $g \approx 2.0$ and $g \approx 3.5$ show significantly lower intensity after heating at 600°C . This decrease might occur due to microheterogeneous regions of $\text{Mn}^{2+}/\text{Mn}^{3+}$ or $\text{Mn}^{2+}/\text{Fe}^{3+}$ clusters, which dif-

fuse out due to heat treatment. After irradiation at 800 kGy , the resonance signal at $g \approx 2.0$ reappeared. This signal could be ascribed to a partial reduction of isolated Mn^{3+} to Mn^{2+} and/or Fe^{2+} to Fe^{3+} due to the e-beam irradiation. Hence, we could tentatively ascribe the pink color of T1 to the Mn and/or Fe ions related to $g \approx 2.0$ signals. The oxidation/reduction behavior of the Mn ion caused by the thermal/e-beam treatments in T1 is rather ambiguous compared to that in T2.

T2 shows a rather different EPR behavior caused to T1. After heating at 600°C , the signal at $g \approx 2.07$ is significantly decreased whilst the signal at $g \approx 3.5$ is slightly increased. This indicates that a magnetically coupling of Mn^{2+} -O- Mn^{3+} or Mn^{2+} -O- Fe^{3+} clusters slightly increases at the partial expense of isolated Mn^{2+} ions ($g \approx 2.07$). The intensities of the six hyperfine lines are also decreased by heating at 600°C . This indicates that the absorption bands at 390 and 520 nm in T2 could originate from the isolated Mn and/or Fe^{3+} ions related with the resonance signal at $g \approx 2.07$. After irradiation with electrons at 800 kGy , the intensities of the two signals, one at $g \approx 2.07$ and the other at $g \approx 3.5$ are increased. Therefore, the pink color in T2 can be ascribed to the isolated Mn and/or Fe ions giving rise to the resonance at $g \approx 2.07$. In addition, the intensity of the six hyperfine lines is slightly increased after the irradiation of 800 kGy .

5. Mid-infrared Spectroscopy

The mid-infrared spectra of the tourmaline gemstone are very sensitive to transition-metal variations [38]. In the OH-stretching region, distinguishing the inner hydroxyl group, with low-intensity bands at high wavenumbers, from the three outer ones, which produce broad high-intensity, low-wavenumber bands, is easy. The high-wavenumber bands ($> 3600\text{ cm}^{-1}$) are particularly sensitive to the X-site occupancy (Na or \square), and to the cation distribution over the adjacent Y sites (Mn^{2+} , Mn^{3+}). The lower wavenumber bands ($3600 - 3300\text{ cm}^{-1}$) reveal the cationic distribution over the Y and the Z sites with great accuracy. The valence state of the Y-cation(s) can be characterized by using the wavenumbers of both the inner and the outer hydroxyl groups. Other studies have also assigned stretching vibrations for tourmaline. The $\nu(\text{BO}_3)$ mode usually appears as a double peak in tourmaline (schorl) at around 1350 and 1250 cm^{-1} [39]. The Si-O and the Si-O-Al vibrations show absorption bands between 1200 and 820 cm^{-1} . Furthermore, the combined stretching and bending modes of the cationic hydroxyl units are observed in the region of $4800 - 4400\text{ cm}^{-1}$. The bending modes of MgOH are observed at 1110 cm^{-1} [16]. However, this absorption band can be assigned to Si-O stretching of different sheets of silicate minerals containing OH groups [40].

Our analyzed spectra were compared to their reported

Table 4. Assignments of the observed mid-infrared absorption bands (3800 – 3400 cm^{-1} and 4800 – 4400 cm^{-1}) of T1, T2, and T3.

Absorption bands range (cm^{-1})	In present work			Reddy <i>et al.</i> [19]		Liu <i>et al.</i> [41]			Assignments		
	T1	T2	T3	Pink	Green	Pink	Green	Brownish -Green			
4800 – 4400	4166	4150	4169		4171	4146	4177	4175	Combination of stretching and bending modes of M-OH	$^Y\text{M-OH}_3$	
			4213	4194				4211		4214	$^Y\text{M-OH}_3$
	4335	4337	4345	4340	4347	4347	4347	4344		$^Z\text{M-OH}_3$	
	4438	4435	4443	4433	4433	4444	4448	4444		$^Y\text{M-OH}_1$	
	4532	4535	4543	4535	4538	4541	4545	4541		$^Y\text{M-OH}_1$	
	4600	4598	4599	4601	4597	4604	4604	4596		$^Y\text{M-OH}_1$	
3800 – 3400	3645		3679	3650	3655	ND	ND	3670	Hydroxyl stretching	$\text{OH}_1\text{-}^Y(\text{Al, Fe, Mn})$	
	3577			3555	3590	ND	ND	3580		$\text{OH}_3\text{-}^Y(\text{Al, Fe, Mn})^Z\text{Al}$	
	3494			3460	3475	ND	ND	3490		$\text{OH}_3\text{-}^Y(\text{Al, Fe, Mn})^Z\text{Al}$	

*ND = No data, blank = no absorption

in the literature. The spectra of all three samples in their natural states were rather similar. T3 had the highest intensity peaks, followed by T2 and T1. The weak bands appeared in range from 2800 to 2500 cm^{-1} , and strong intensity bands appeared in range from 3000 to 3750 cm^{-1} . The moderately intense bands appeared around 4800 – 4400 cm^{-1} . These absorption bands will be discussed in relation with the results obtained by Reddy *et al.* [19], who assigned the bands in this range to the combined of the stretching and bending modes of cationic hydroxyl units (MOH, where M is Al, Mg, Fe, Mn, *etc.*).

The absorption band (E \perp c) of samples T1, T2, and T3 in the 4800 – 4000 cm^{-1} region before and after treatment are shown in Figs. 6(a), (b), and (c), respectively. All samples exhibited similar behaviors, showing absorption bands near 4600, 4530, 4440, and 4340 cm^{-1} and between 4300 – 4100 cm^{-1} . The combined of the stretching and bending modes of $^Y\text{M-OH}_1$ commonly lead to bands at 4600, 4530, and 4440 cm^{-1} . Changes in the intensities of the absorption bands intensity at each step of the treatment indicated that the combination bands of the $^Y\text{M-OH}_1$ units are affected slightly by ^YM metallic ions due to the hydroxyl groups at *W* sites. The intensity increase of these bands after heating indicates that the bond distances between the metal ions and the hydroxyl group have changed. All samples showed increased in intensities for the bands at 4600, 4530 and 4440 cm^{-1} after heating at 600 $^\circ\text{C}$. The intensity was decreased after subsequent e-beam irradiation at 800 kGy. The absorption bands at 4600 cm^{-1} are suggested to be combination bands involving Al-OH units [19]. Therefore, the absorption bands near 4600 cm^{-1} are considered to be the combination bands involving $^Y\text{Al-OH}_1$. The combination band observed near 4340 cm^{-1} occurs due to a combination of the stretching and the bending modes of $^Z\text{M-OH}_3$ [41]. The *Z* sites in the three elbaite samples are mainly occupied by Al^{3+} . Therefore, the $^Z\text{M-OH}_3$

units are mainly constituted of $^Z\text{Al-OH}_3$. Similar with those bands, the intensity of the band near 4340 cm^{-1} band is increased after heating and is decreased after subsequent irradiation with electrons. The two bands in the range of 4300 – 4100 cm^{-1} are considered to be due to a combination of the stretching and bending modes of $^Y\text{M-OH}_3$, in which the units are much complex, having many types of metallic ions located at *Y* sites. Of the assignments of the three absorption bands reported in the literature, the two samples from Reddy *et al.* [19] and the three samples from Liu *et al.* [41] are discussed in Table 4.

The T1 sample showed the most drastic decrease in the intensities of the bands at 4600, 4530, 4440 and 4340 cm^{-1} after having been irradiated with an e-beam at electron 800 kGy. This intensity decrease indicates a decomposition of the OH^- group into O^- (hole trap) and H° (electron trap), resulting in a decrease in the intensity. However, the decomposition phenomenon was less severe in T2 and T3. Hence, only T1 was changed to a yellow color by e-beam irradiation. In T1, after heating and subsequent irradiation with electron, electron and hole traps (color centers) are the main cause of color while the existence of Mn^{2+} and Mn^{3+} in T2 cause its pink color.

Figure 7 shows the spectra in the range of 3850 – 3350 cm^{-1} for the three samples. These bands are considered to be hydroxyl stretching modes [13, 19, 42]. The absorption bands at 3490 and 3578 cm^{-1} are assigned to the stretching modes of the $-\text{OH}_3$ groups whereas the band at 3671 cm^{-1} is attributed to the stretching modes of the $-\text{OH}_1$ groups. Those three absorption bands are clearly visible in T1 whereas they do not appear in T2; only the absorption band at around 3680 cm^{-1} appears in T3. The intensity change of these absorption bands after treatment is related to the distance between the metal ions and the hydroxyl groups. In this research,

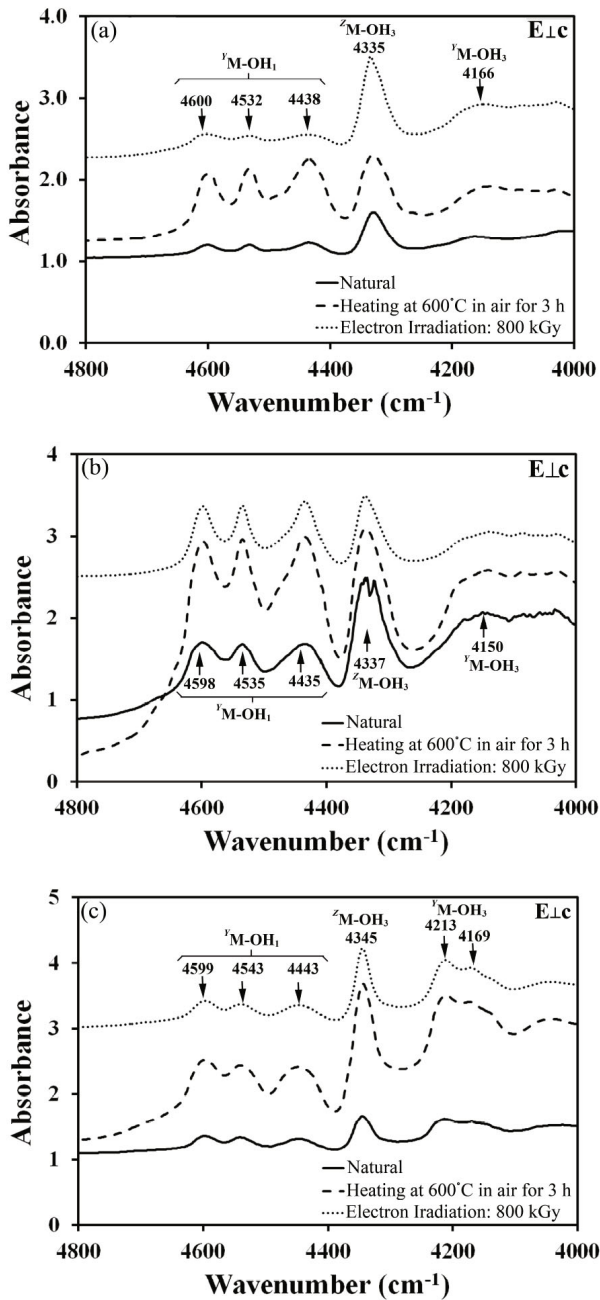


Fig. 6. Mid-infrared spectra in the 4800 – 4000 cm^{-1} region for (a) T1, (b) T2 and (c) T3.

the assignments for the absorption bands in the three samples were compared to one another, as well as to the assignments given to the green sample by Liu *et al.* [41], and the results are shown in Table 4.

IV. CONCLUSION

Pink tourmalines became colorless when heated at 600 °C. The pink tourmaline with higher manganese content

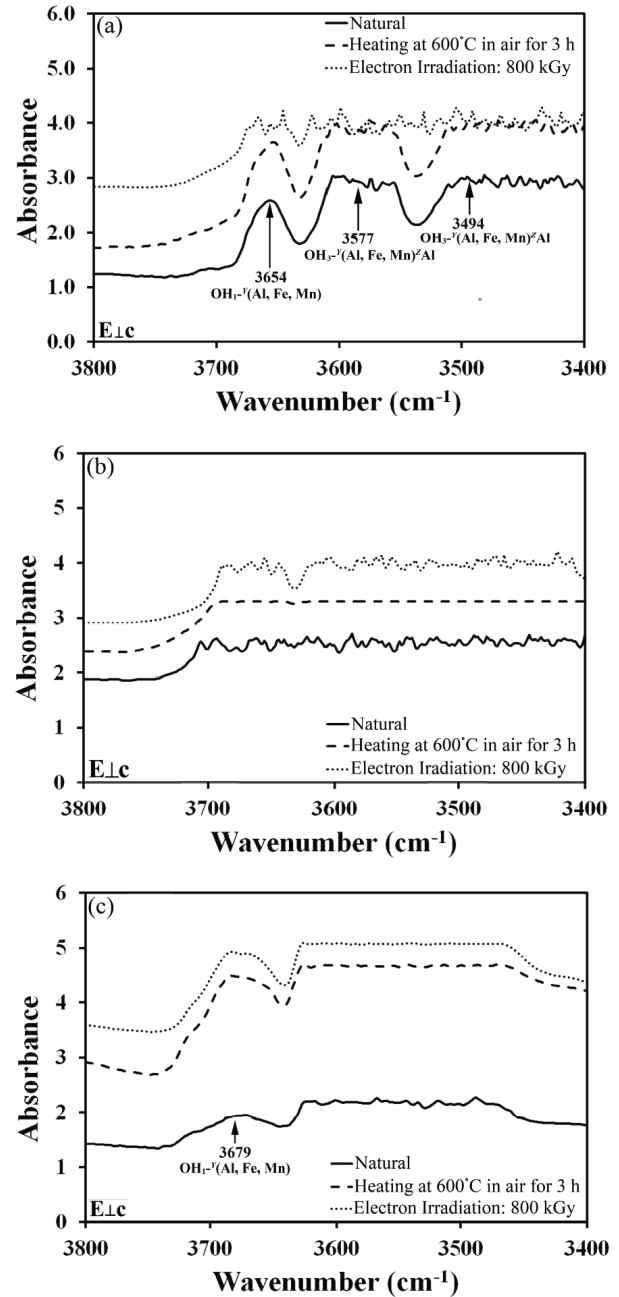


Fig. 7. Mid-infrared spectra in the 3800 – 3400 cm^{-1} region for (a) T1, (b) T2 and (c) T3.

could recover its pink color by electron irradiation. This is ascribed to the partial oxidation/reduction reaction of isolated Mn ions simultaneously with Fe ions. The EPR spectra indicated two types of environments for Mn ions: isolated and clustered states. Mid-infrared spectra in the ranges of 3800 – 3400 cm^{-1} and 4800 – 4000 cm^{-1} are related to hydroxyl stretching modes. Heat treatment and electron irradiation affect the stretching modes of Y M metallic ions. The T1 showed the most drastic decrease in intensity of the bands at 4600, 4530, 4440 and

4340 cm^{-1} after having been irradiated with electrons at 800 kGy. The decomposing of the OH^- groups into O^- (hole trap) and Ho (electron trap) resulted in a decrease in the intensity. This decomposition resulted in the yellow color in T1. The decomposition phenomenon was less severe in T2 and T3. Hence, only T1 were changed to yellow by e-beam irradiation. Heating and electron irradiation did not affect the color of the green tourmaline. Heat treatment and irradiation (electron or gamma ray) can be effective methods for color enhancement of the tourmaline. The color change may occur through different mechanisms depending on, most of all, the composition of tourmaline. It also depends on conditions such as the temperature and the duration of heat treatment, the dose and the type of irradiation, the procedure of irradiation and heat treatment, and the quantity of impurities present in the mineral.

ACKNOWLEDGMENTS

The authors would like to thank Anankitphatana Pasit and Azizi Enterprises Co., Ltd., for providing the samples. In addition, for sample preparations and EDXRF analyses, we are grateful to Makakum Chanida. Panyanuch Adisak, the head of the radiation machine management division at the Gems Irradiation Center, Thailand Institute of Nuclear Technology (TINT), including staff members, namely, Panomwong Saruda, Jangswang Nongnuch, and Charoennam Tasanee, is to provide the indispensable process of electron beam irradiation.

REFERENCES

- [1] P. S. R. Prasad and D. Srinivasa Sarma, *Gondzvana Res.* **8**, 265 (2005).
- [2] F. C. Hawthorne and D. J. Henry, *Eur. J. Mineral.* **11**, 201 (1999).
- [3] L. V. Bershov, V. O. Martirosyan, A. S. Marfunin, A. N. Platonov and A. N. Tarashehan, *Sov. Phys. Crystallogr.* **13**, 629 (1969).
- [4] K. Nassau, *Am. Mineral.* **60**, 710 (1975).
- [5] C. Castañeda, S. G. Eeckhout, G. M. da Costa, N. F. Botelho and E. De Grave, *Phys. Chem. Minerals* **33**, 207 (2006).
- [6] P. Baěík, D. Ozdín, M. Miglierini, P. Kardošová, M. Penetrák and J. Haloda, *Phys. Chem. Minerals* **38**, 599 (2011).
- [7] S. C. Lind and D. C. Bardwell, *Am. Mineral.* **9**, 678 (1923).
- [8] F. H. Pough and T. H. Rogers, *Am. Mineral.* **32**, 31 (1947).
- [9] P. G. Manning, *Can. Mineral.* **9**, 678 (1969).
- [10] K. Nassau, *Lapidary J.* **28**, 1064 (1974).
- [11] G. H. Faye, P. G. Manning, J. R. Gosselin and R. J. Tremblay, *Can. Mineral.* **8**, 171 (1974).
- [12] M. B. De Camargo and S. Isotani, *Am. Mineral.* **73**, 172 (1988).
- [13] I. M. Reinitz and G. R. Rossman, *Am. Mineral.* **73**, 822 (1988).
- [14] I. Petrov, *Am. Mineral.* **75**, 237 (1990).
- [15] B. M. Laurs, J. C. Zwaan, C. M. Breeding, W. B. Simmons, D. Beaton, K. F. Rijdsdijk, R. Befi and A. U. Falster, *Gem. Gemol.* **44**, 4 (2008).
- [16] Y. Ahn, J. Seo and J. Park, *Vib. Spec.* **65**, 165 (2013).
- [17] P. G. Manning, *Can. Mineral.* **11**, 971 (1973).
- [18] G. R. Rossman and S. M. Mattson, *Am. Mineral.* **71**, 599 (1986).
- [19] B. J. Reddy, R. L. Frost, W. N. Martens, D. L. Wain and J. T. Klopogge, *Vib. Spectrosc.* **44**, 42 (2007).
- [20] D. M. Sherman and N. Vergo, *Am. Mineral.* **73**, 140 (1988).
- [21] S. M. Mattson, Dissertation (Ph.D.), California Institute of Technology, 1985.
- [22] K. Krambrock, M. V. B. Pinheiro, S. M. Medeiros, K. J. Guedes, S. Schweizer and J. M. Spaeth, *Nucl. Instrum. Meth. B* **191**, 241 (2002).
- [23] G. H. Faye, P. G. Manning and E. H. Nickel, *Amer. Mineral.* **53**, 1174 (1968).
- [24] S. M. Mattson and G. R. Rossman, *Phys. Chem. Minerals* **14**, 163 (1987).
- [25] G. R. Rossman, E. Fritsch and J. E. Shigley, *Am. Mineral.* **76**, 1479 (1991).
- [26] G. Smith, *Phys. Chem. minerals* **3**, 375 (1978).
- [27] A. Abragam and B. Bleaney, *Electron Paramagnetic Resonance of Transition Ions* (Clarendon Press, Oxford, 1970), Chap. 1, p. 9.
- [28] P. L. Hall, *Clay. Miner.* **15**, 321 (1980).
- [29] N. Srisittipokakun, C. KedKaew, J. Kaewkhao, T. Kit-tiauchawal, K. Thamaphat and P. Limsuwan, *Kasetsart J. (Nat. Sci.)* **43**, 360 (2009).
- [30] R. P. S. Chakradhar, G. Sivaramaiah, J. L. Rao and N. O. Gopal, *Spectrochim. Acta, Part A* **62**, 761 (2005).
- [31] L. B. Glebov, L. N. Glebova, D. E. Jones and R. R. Rakhimov, *Non-crystalline Solids* **265**, 181 (2000).
- [32] R. P. S. Chakradhar, K. P. Ramesh, J. L. Rao and J. Ramakrishna, *J. Phys. Chem. Solids* **64**, 641 (2003).
- [33] R. S. Muralidharaa, C. R. Kesavulub, J. L. Raob, R. V. Anavekara and R. P. S. Chakradhar, *J. Phys. Chem. Solids* **71**, 1651 (2010).
- [34] R. P. S. Chakradhar, A. Murali and J. L. Rao, *Opt. Mater.* **10**, 109 (1998).
- [35] S. O. Souza, G. M. Ferraz and S. Watanabe, *Nucl. Instr. Meth. Phys. Res. B* **218**, 259 (2004).
- [36] J. Babińska, K. Dyrek, A. Pieczka and Z. Sojka, *Eur. J. Mineral.* **20**, 233 (2008).
- [37] S. P. Chaudhuri and S. K. Patra, *J. Mater. Sci.* **35**, 4735 (2000).
- [38] T. Gonzalez-Carrefio, M. Fernandez and J. Sanz, *Phys. Chem. Minerals* **15**, 452 (1988).
- [39] P. Makreski and G. Jovanovski, *Spectrochim. Acta Part A* **73**, 460 (2009).
- [40] V. Sontevska, G. Jovanovski and P. Makreski, *J. Mol. Struct.* **834**, 318 (2007).
- [41] X. Liu, X. Feng, J. Fan and S. Guo, *Chin. Opt. Lett.* **9**, 083001 (2011).
- [42] D. Cao, G. Zhao, Q. Dong, J. Chen, Y. Cheng, Y. Ding and J. Zou, *Chin. Opt. Lett.* **8**, 199 (2010).